modulus (c) imaginary part of the modulus. The frequency is 312.5 kHz and $\lambda_0 =$ 4.8 mm. The reconstruction area is $14\lambda_0 \times 14\lambda_0$ and divided into 127×127 cells. 128×102 transmitter/receiver paired data are used.

Figure 9. The dual-balloon images for iteration 8: (a) density (b) real part of the modulus (c) imaginary part of the modulus. The frequency is 312.5 kHz and $\lambda_0 =$ 4.8 mm. The reconstruction area is $14\lambda_0 \times 14\lambda_0$ and divided into 127×127 cells. 128×102 transmitter/receiver paired data are used.

Figure 10. Comparison of the dual-balloon reconstructions for iteration 1 and iteration 8. The frequency is 312.5 kHz and $\lambda_0 = 4.8$ mm. The reconstruction area is $14\lambda_0 \times 14\lambda_0$ and divided into 127×127 cells. 128×102 transmitter/receiver paired data are used.

Figure 11. Density images of a boiled egg for iteration 1 and 2. The frequency is 468.75 kHz and $\lambda_0 = 3.2$ mm. The reconstruction area is $18.14\lambda_0 \times 18.14\lambda_0$ and divided into 181×181 cells. 256×205 transmitter/receiver paired data are used. Two apparent points residing at the left of the figure and the center of the egg correspond to the tank origin and the mounting hole respectively. A wire scar slantly extends from the lower left of the egg toward to the egg's right edge.

Figure 12. The real part of the modulus images of a boiled egg for iteration 1 and 2. The frequency is 468.75 kHz and $\lambda_0 = 3.2$ mm. The reconstruction area is $18.14\lambda_0 \times 18.14\lambda_0$ and divided into 181×181 cells. 256×205 transmitter/receiver paired data are used. Two apparent points residing at the left of the figure and the center of the egg correspond to the tank origin and the mounting hole respectively. A wire scar slantly extends from the lower left of the egg toward to the egg's right edge.

Figure 13. The imaginary part of the modulus images of a boiled egg for iteration 1 and 2. The frequency is 468.75 kHz and $\lambda_0 = 3.2$ mm. The reconstruction area is $18.14\lambda_0 \times 18.14\lambda_0$ and divided into 181×181 cells. 256×205 transmitter/receiver paired data are used. Two apparent points residing at the left of the figure and the center of the egg correspond to the tank origin and the mounting hole respectively. The wire scar is not observable in this image.

Figure 14. Plots of the x-axis cross section through the center for iteration 1 and 2. The frequency is 468.75 kHz and $\lambda_0 = 3.2$ mm. The reconstruction area is $18.14\lambda_0 \times 18.14\lambda_0$ and divided into 181×181 cells. 256×205 transmitter/receiver paired data are used.

Figure 15. The maximal N_i for a certain N such that the cost for the direct matrix-vector multiplies ($O(N^2)$) would be larger than that for solving numerous forward scattering problems ($O(N_i N^{1.5} \log N)$).

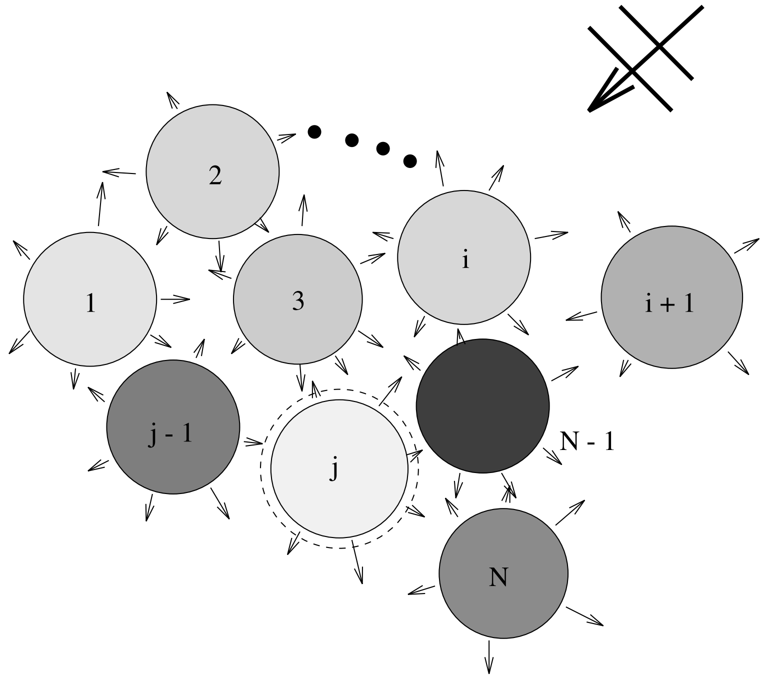

Figure 1. Multiple scattering from N subscatterers. The total field impinging on the j-th subscatterer consists of the incident field and all scattered fields from the other subscatterers.

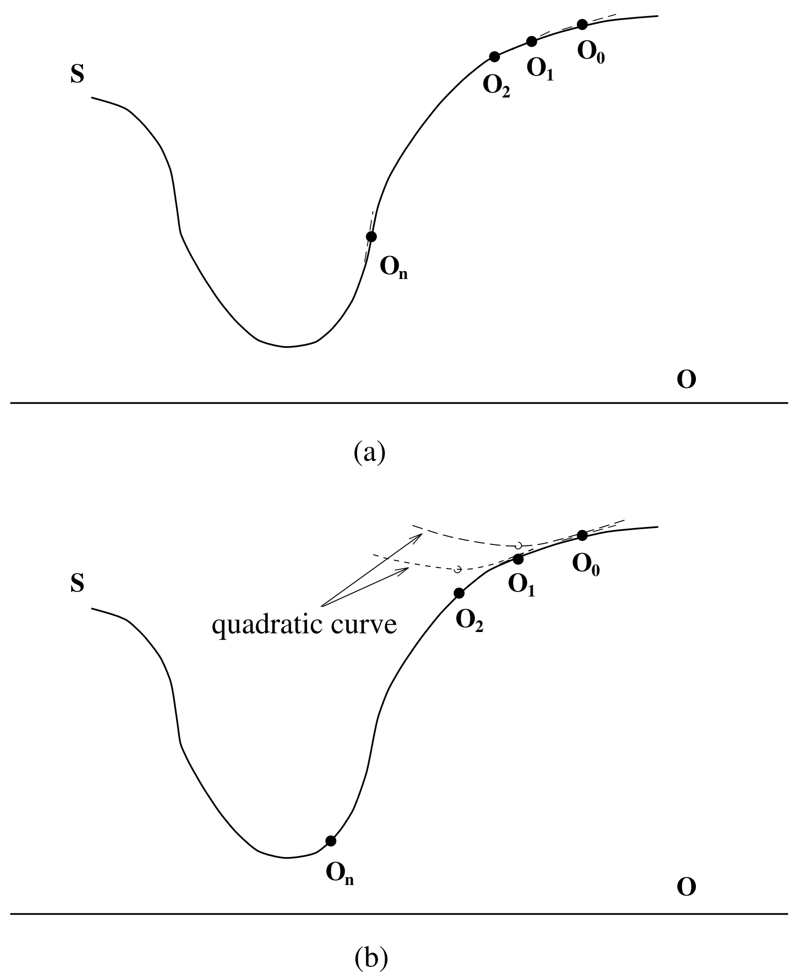

Figure 2. (a) The conjugate gradient minimization scheme; (b) the distorted Born iterative method.

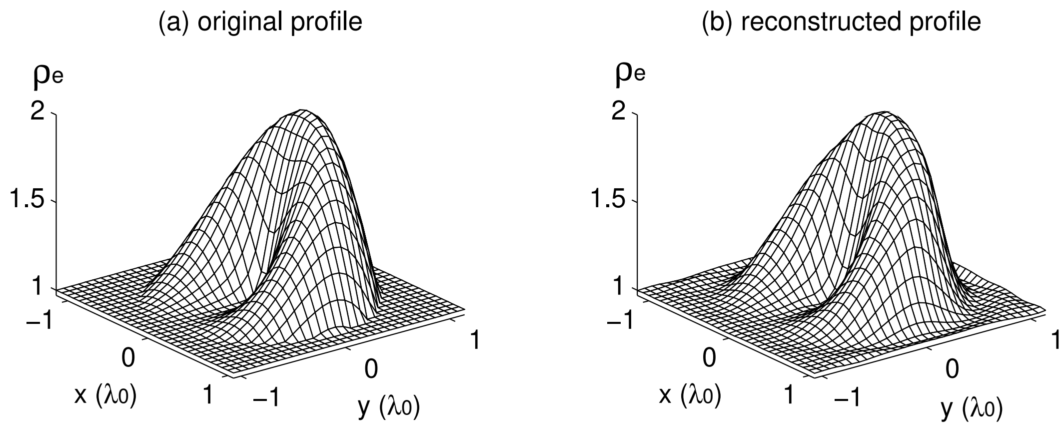

Figure 3. The true and reconstructed density profiles (no compressibility variation). The reconstructed area is $2.26\lambda_0 \times 2.26\lambda_0$ and is divided into a 32×32 mesh. There are 16 transmitters and 32 receivers.

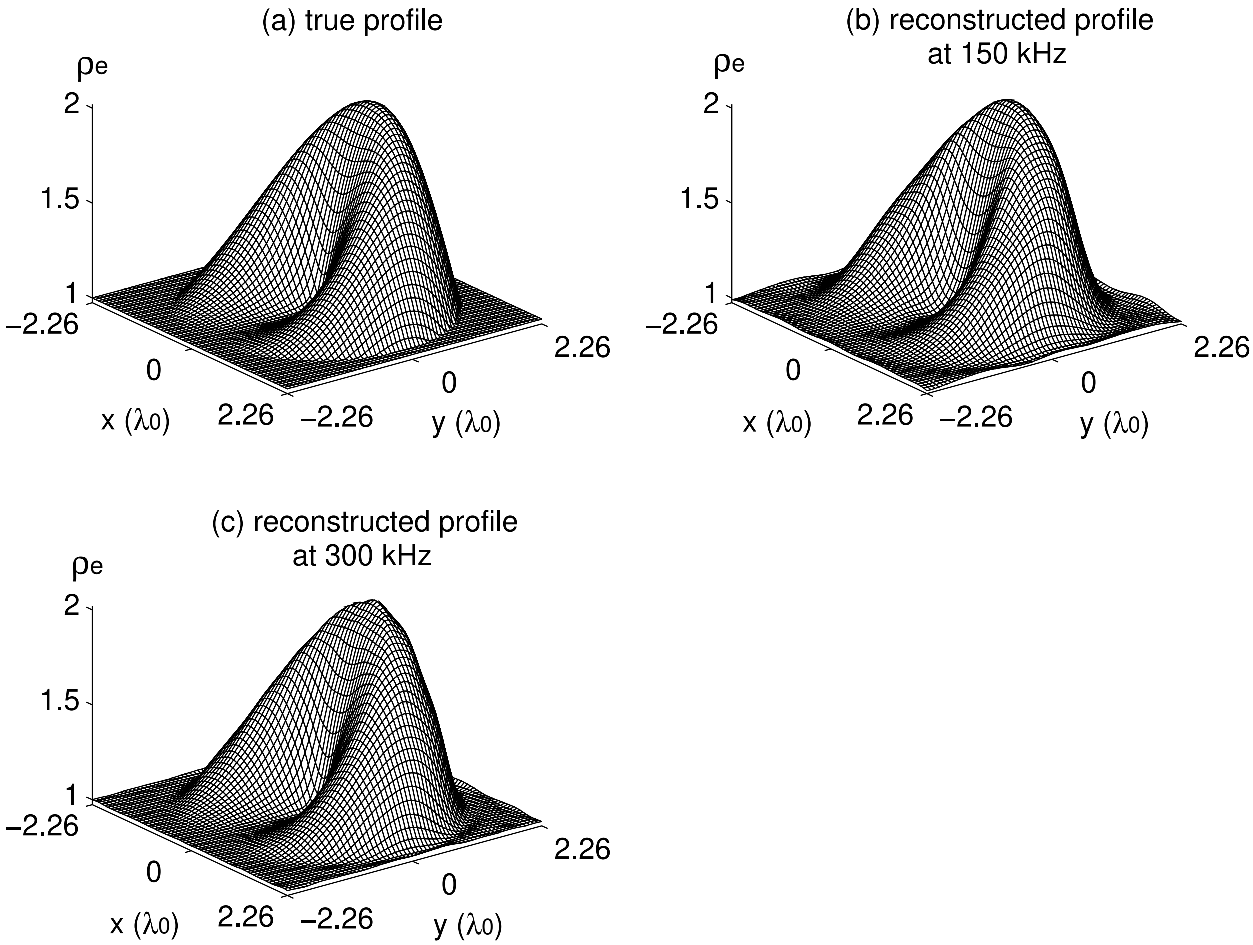

Figure 4. The true and reconstructed density profiles (no compressibility variation) by the frequency-hopping scheme. The reconstructed area is $4.52\lambda_0 \times 4.52\lambda_0$ (background wavelength at 300 kHz) and is divided into a 64×64 mesh. There are 32 transmitters and 64 receivers.

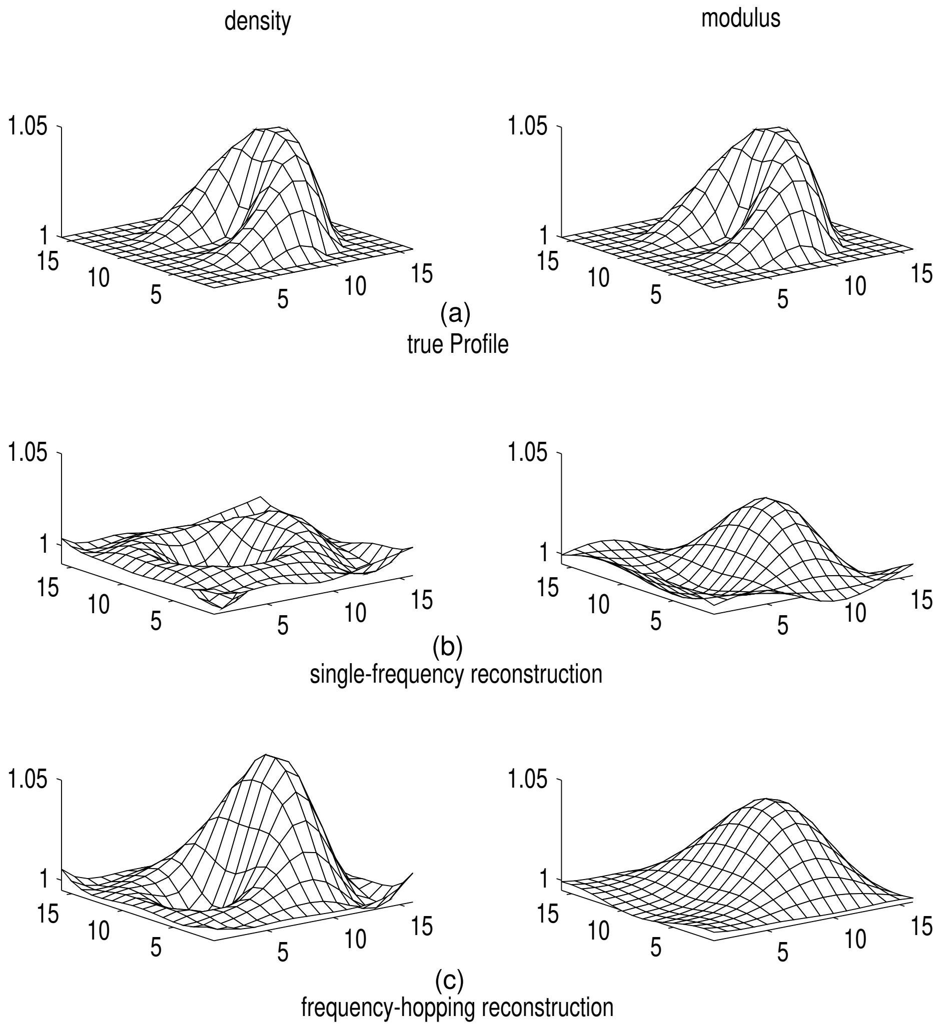

Figure 5. The true and reconstructed profiles in the density and modulus. The reconstructed area is $1\lambda_0 \times 1\lambda_0$ and divided into a 16×16 mesh. There are 16×15 sets of measurement data. 150 kHz, 225 kHz and 300 kHz are used in the frequency-hopping scheme.

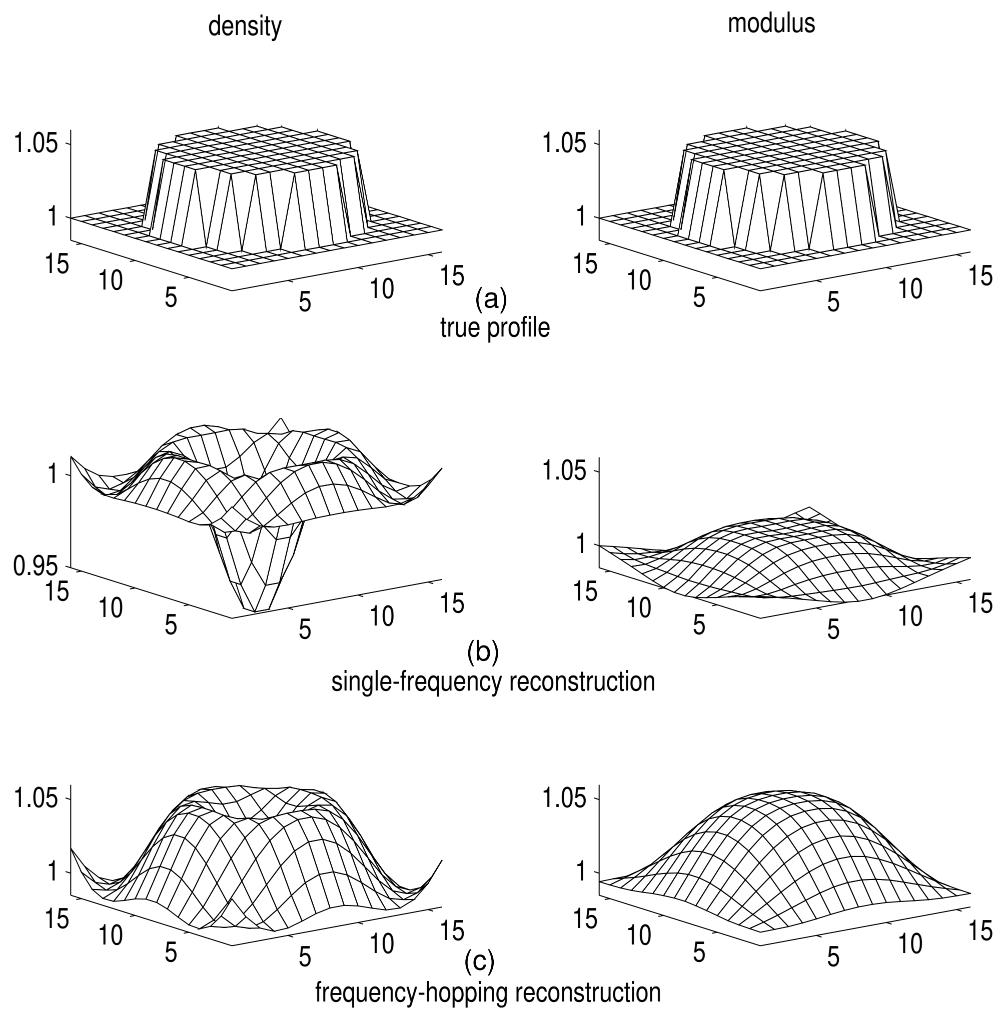

Figure 6. The true and reconstructed profiles in the density and modulus. The reconstructed area is $1\lambda_0 \times 1\lambda_0$ and divided into a 16×16 mesh. There are 16×15 sets of measurement data. 150 kHz, 225 kHz and 300 kHz are used in the frequency-hopping scheme.

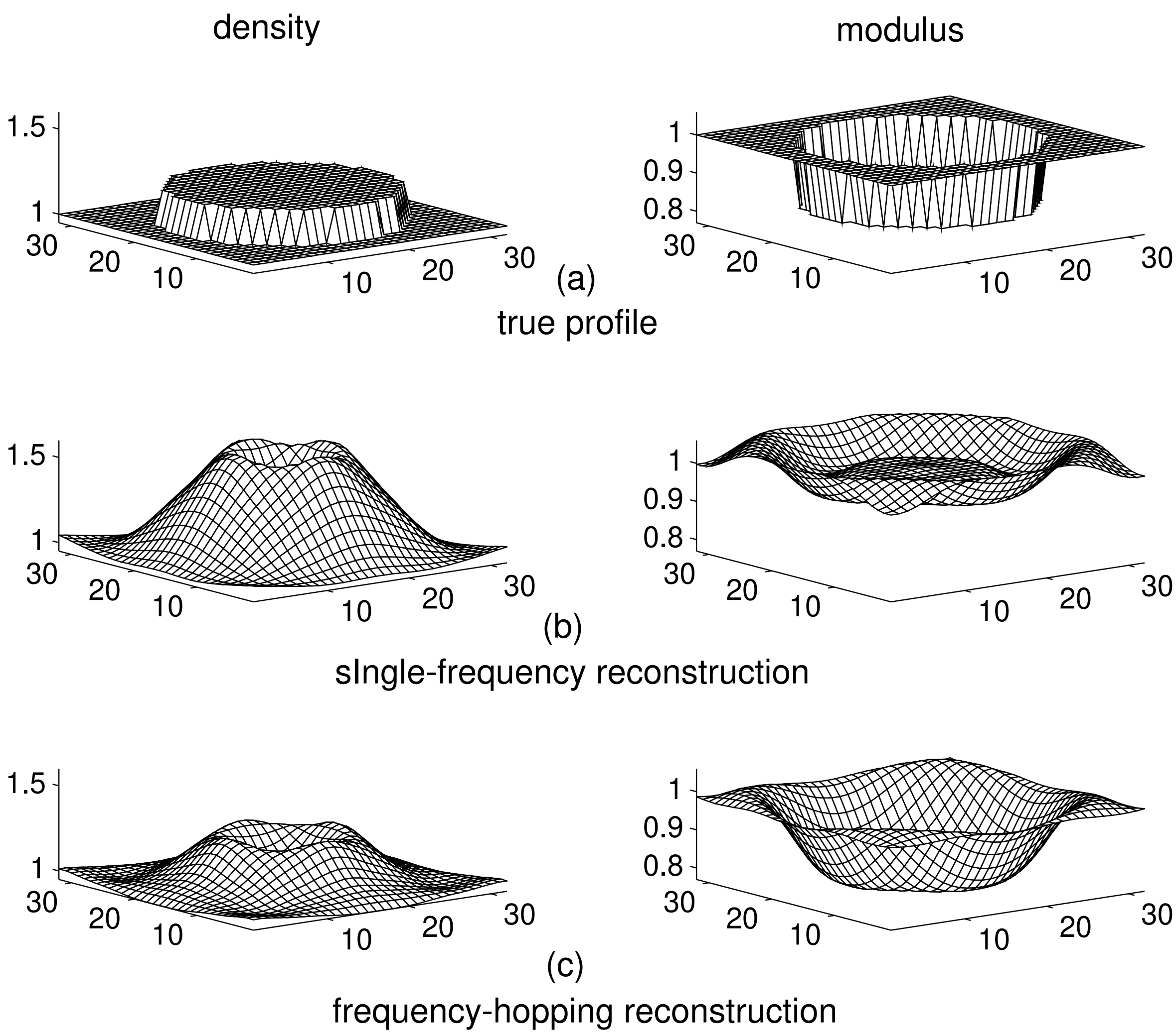

Figure 7. The true and reconstructed profiles in the density and modulus. The reconstructed area is $2\lambda_0 \times 2\lambda_0$ and divided into a 32×32 mesh. There are 32×31 sets of measurement data. 300 kHz, 600 kHz, 1.2 MHz and 2.4 MHz are used in the frequency-hopping scheme.

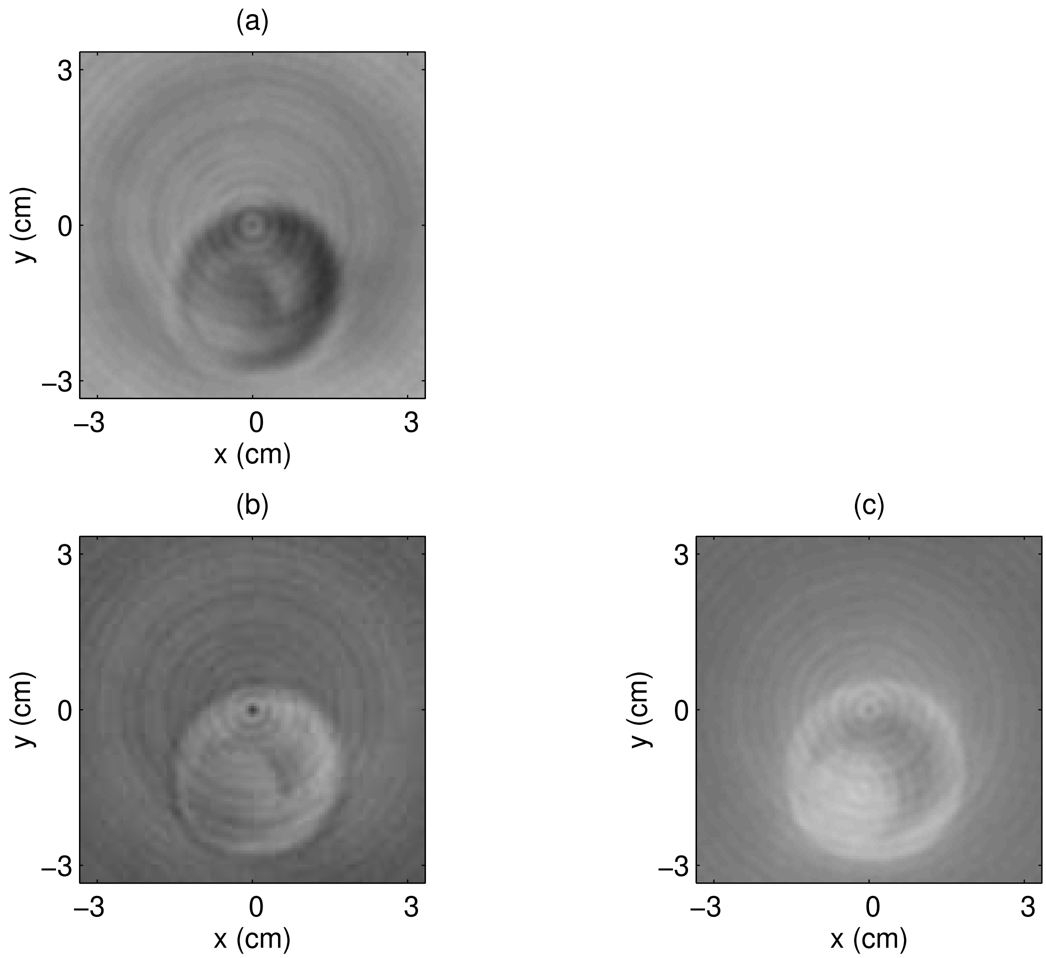

Figure 8. The dual-balloon images for iteration 1: (a) density (b) real part of the modulus (c) imaginary part of the modulus. The frequency is 312.5 kHz and $\lambda_0 = 4.8$ mm. The reconstruction area is $14\lambda_0 \times 14\lambda_0$ and divided into 127×127 cells. 128×102 transmitter/receiver paired data are used.

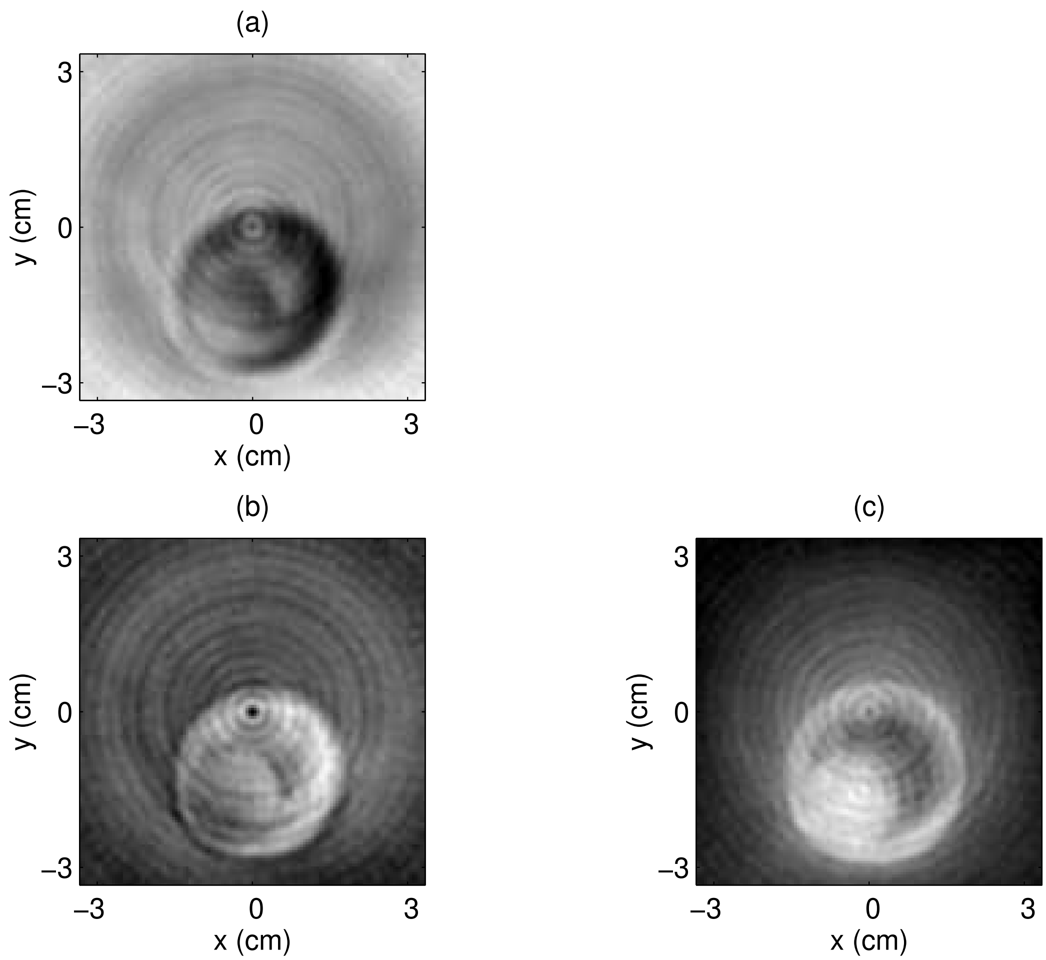

Figure 9. The dual-balloon images for iteration 8: (a) density (b) real part of the modulus (c) imaginary part of the modulus. The frequency is 312.5 kHz and $\lambda_0 = 4.8$ mm. The reconstruction area is $14\lambda_0 \times 14\lambda_0$ and divided into 127×127 cells. 128×102 transmitter/receiver paired data are used.

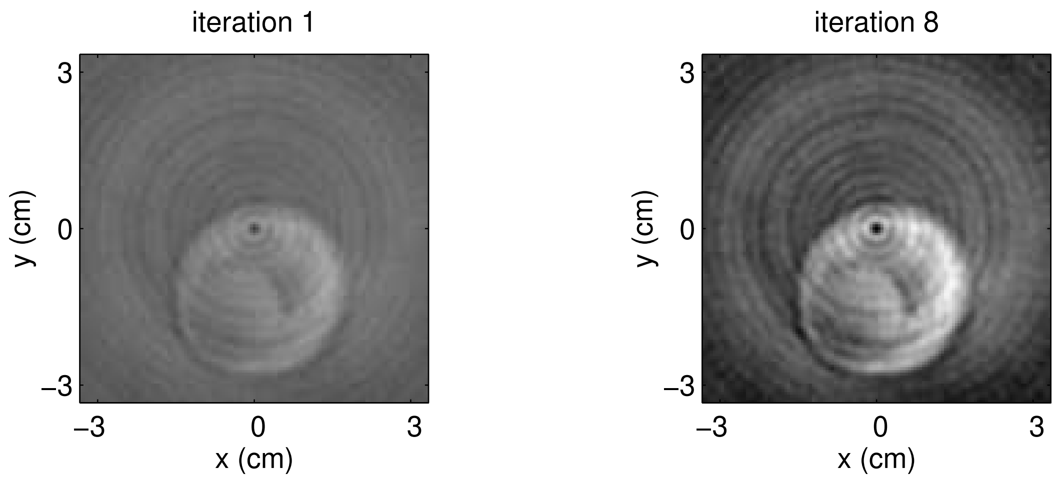

(a) images of the real part of the modulus

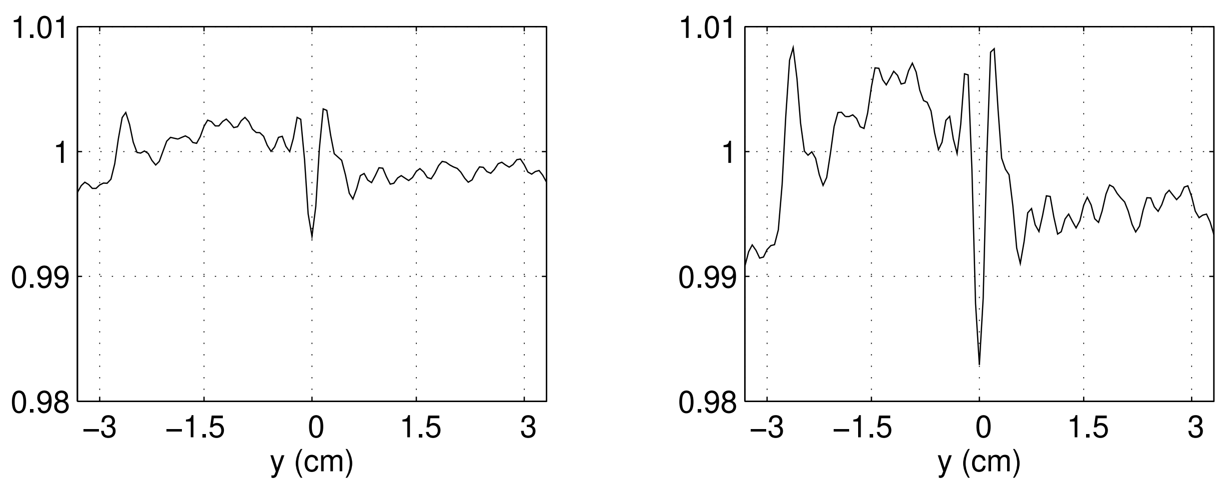

(b) y-axis cross sections of the modulus

Figure 10. Comparison of the dual-balloon reconstructions for iteration 1 and iteration 8. The frequency is 312.5 kHz and $\lambda_0 = 4.8$ mm. The reconstruction area is $14\lambda_0 \times 14\lambda_0$ and divided into 127×127 cells. 128×102 transmitter/receiver paired data are used.

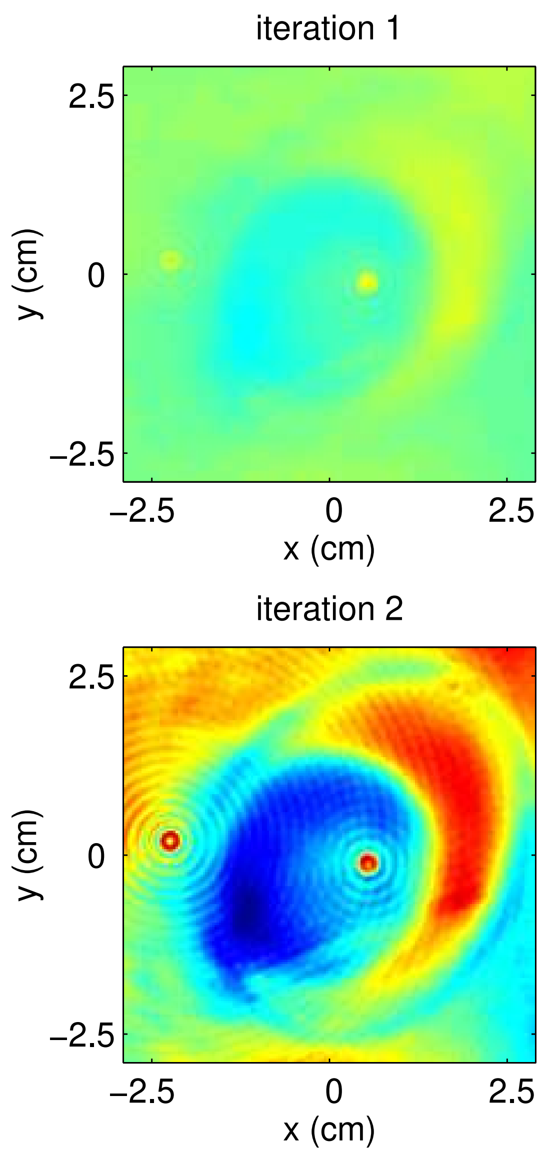

Figure 11. Density images of a boiled egg for iteration 1 and 2. The frequency is 468.75 kHz and $\lambda_0 = 3.2$ mm. The reconstruction area is $18.14\lambda_0 \times 18.14\lambda_0$ and divided into 181×181 cells. 256×205 transmitter/receiver paired data are used. Two apparent points residing at the left of the figure and the center of the egg correspond to the tank origin and the mounting hole respectively. A wire scar slantly extends from the lower left of the egg toward to the egg's right edge.

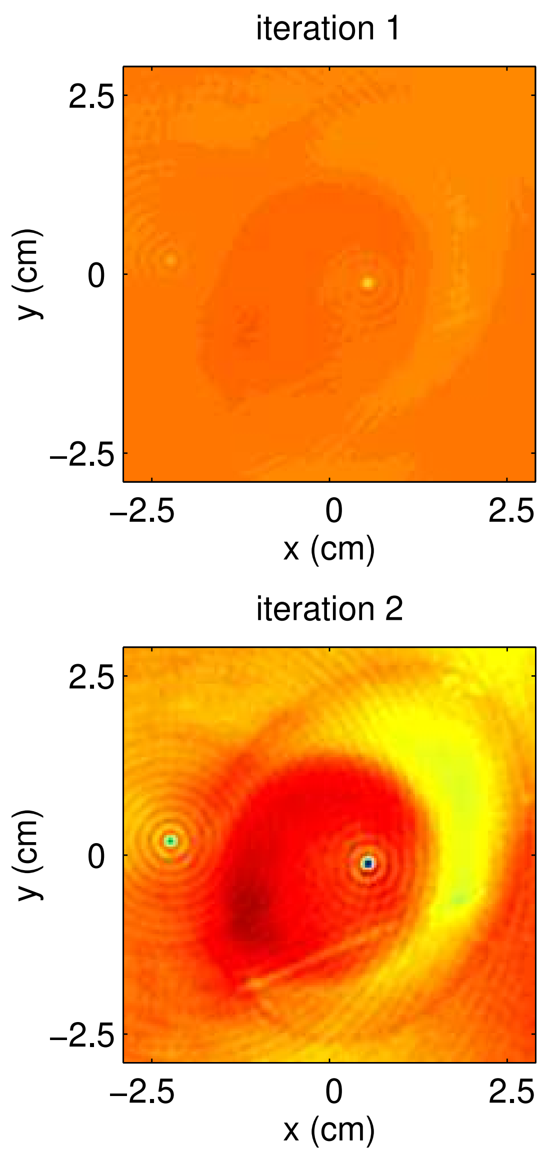

Figure 12. The real part of the modulus images of a boiled egg for iteration 1 and 2. The frequency is 468.75 kHz and $\lambda_0 = 3.2$ mm. The reconstruction area is $18.14\lambda_0 \times 18.14\lambda_0$ and divided into 181×181 cells. 256×205 transmitter/receiver paired data are used. Two apparent points residing at the left of the figure and the center of the egg correspond to the tank origin and the mounting hole respectively. A wire scar slantly extends from the lower left of the egg toward to the egg's right edge.

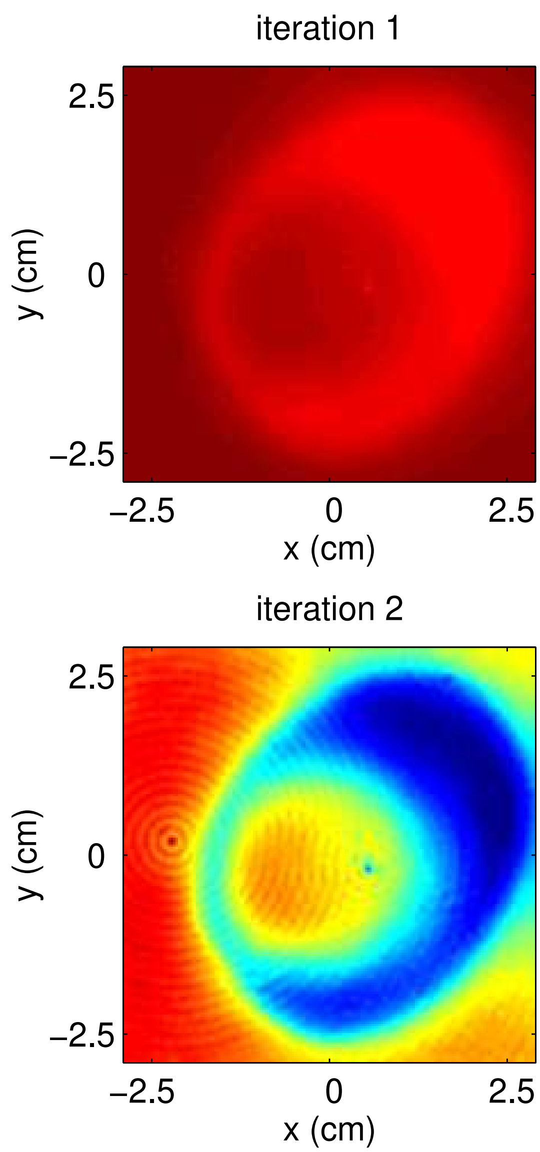

Figure 13. The imaginary part of the modulus images of a boiled egg for iteration 1 and 2. The frequency is 468.75 kHz and $\lambda_0 =$ 3.2 mm. The reconstruction area is $18.14\lambda_0 \times 18.14\lambda_0$ and divided into 181×181 cells. 256×205 transmitter/receiver paired data are used. Two apparent points residing at the left of the figure and the center of the egg correspond to the tank origin and the mounting hole respectively. The wire scar is not observable in these images.

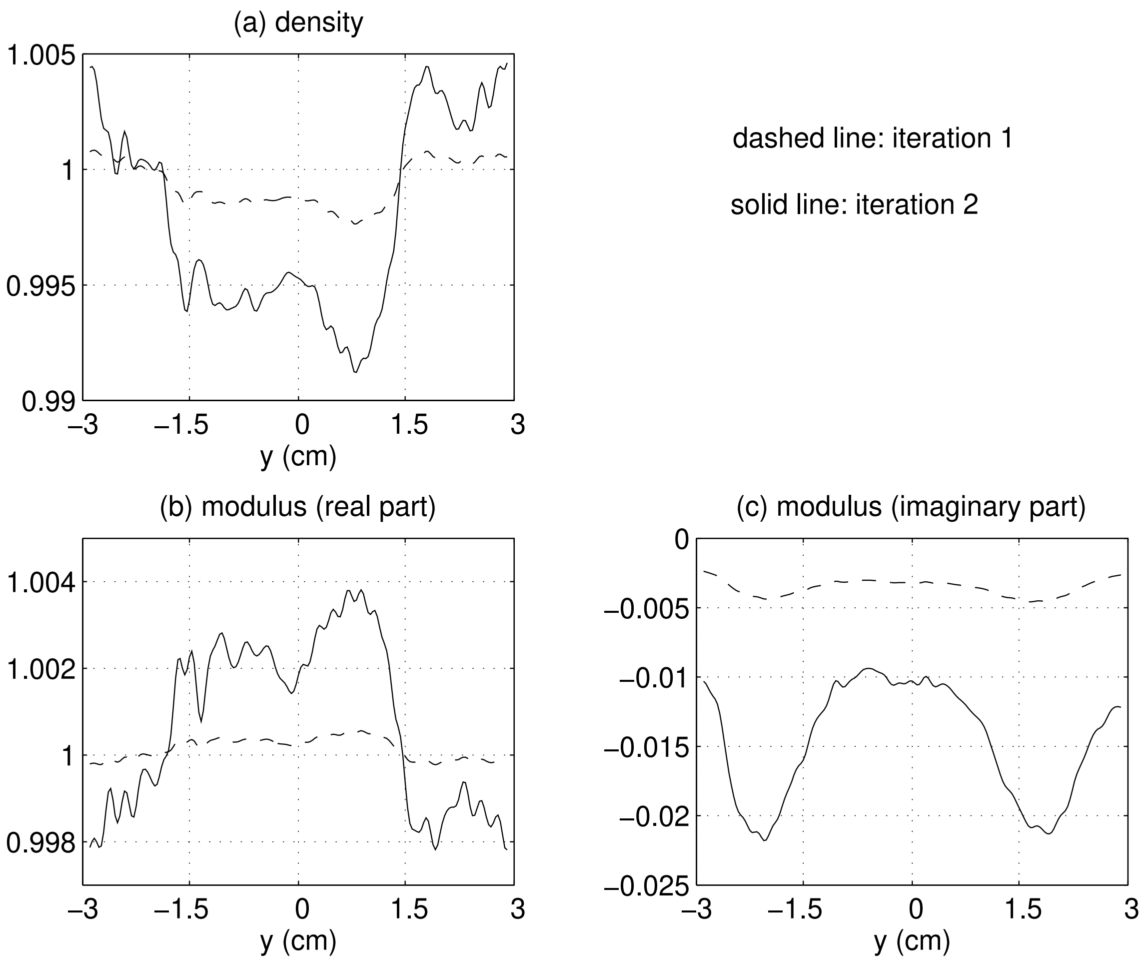

Figure 14. Plots of the x-axis cross section through the center for iteration 1 and 2. The frequency is 468.75 kHz and $\lambda_0 = 3.2$ mm. The reconstruction area is $18.14\lambda_0 \times 18.14\lambda_0$ and divided into 181×181 cells. 256×205 transmitter/receiver paired data are used.

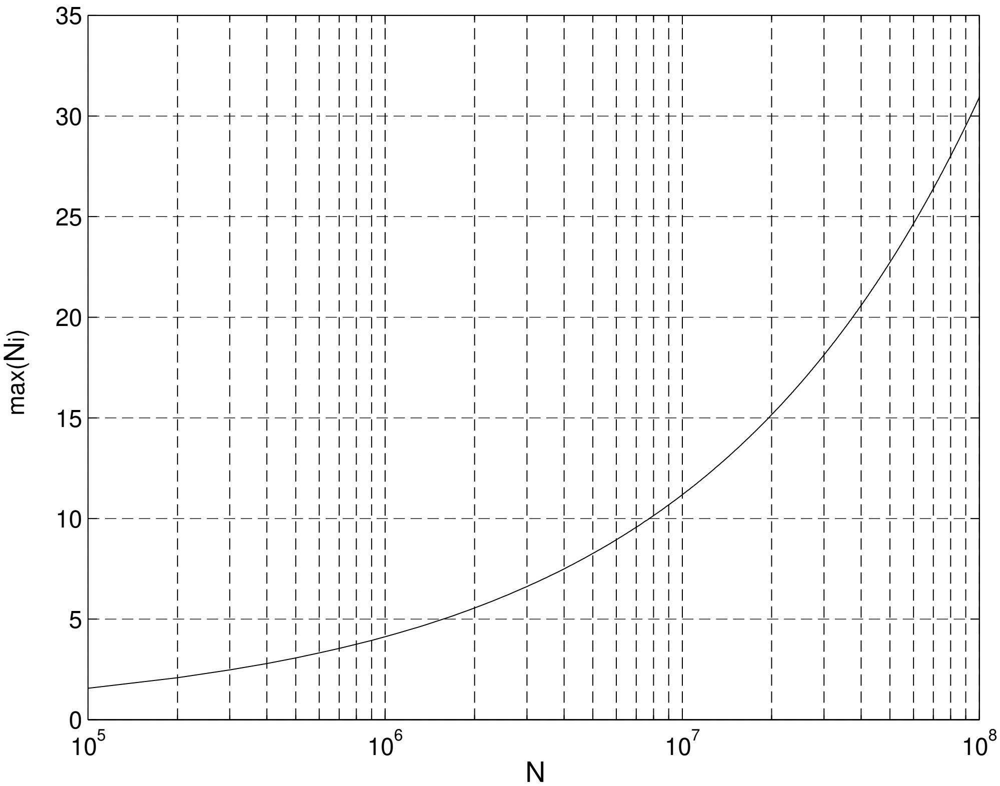

Figure 15. The maximal N_i for a certain N such that the cost for the direct matrix-vector multiplies ($O(N^2)$) would be larger than that for solving numerous forward scattering problems ($O(N_i N^{1.5} \log N)$).